

MIT Open Access Articles

Mechanism of Nitric Oxide Reactivity and Fluorescence Enhancement of the NO-Specific Probe CuFL1

The MIT Faculty has made this article openly available. **Please share** how this access benefits you. Your story matters.

Citation: McQuade, Lindsey E., Michael D. Pluth, and Stephen J. Lippard. "Mechanism of Nitric Oxide Reactivity and Fluorescence Enhancement of the NO-Specific Probe CuFL1." *Inorganic Chemistry* 49.17 (2010): 8025-8033.

As Published: <http://dx.doi.org/10.1021/ic101054u>

Publisher: American Chemical Society

Persistent URL: <http://hdl.handle.net/1721.1/67689>

Version: Author's final manuscript: final author's manuscript post peer review, without publisher's formatting or copy editing

Terms of Use: Article is made available in accordance with the publisher's policy and may be subject to US copyright law. Please refer to the publisher's site for terms of use.



Mechanism of Nitric Oxide Reactivity and Fluorescence

Enhancement of the NO-Specific Probe, CuFL1

*Lindsey E. McQuade, Michael D. Pluth, and Stephen J. Lippard**

Contribution from the Department of Chemistry, Massachusetts Institute of Technology, Cambridge,
Massachusetts 02139

Email: lippard@mit.edu

RECEIVED DATE

TITLE RUNNING HEAD: Mechanism of NO reaction with CuFL1

ABSTRACT: The mechanism of the reaction of CuFL1 (FL1 = 2-{2-chloro-6-hydroxy-5-[(2-methylquinolin-8-ylamino)-methyl]-3-oxo-3*H*-xanthen-9-yl}benzoic acid) with NO to form the *N*-nitrosated product FL1-NO in buffered aqueous solutions was investigated. The reaction is first order in the concentrations of CuFL1, NO, and hydroxide ion. Rate saturation at high base concentrations is consistent with a mechanism in which the protonation state of the secondary amine of the ligand is important for reactivity. This information provides a rationale for designing faster-reacting probes by lowering the pK_a of the secondary amine. Activation parameters for the reaction of CuFL1 with NO indicate an associative mechanism ($\Delta S^\ddagger = -29 \pm 3$ cal/K·mol) with a modest thermal barrier ($\Delta H^\ddagger = 9.7 \pm 0.5$ kcal/mol; $E_a = 10.3 \pm 0.5$ kcal/mol). Variable pH EPR experiments reveal that, as the secondary amine of CuFL1 is deprotonated, electron density shifts to yield a new spin-active species having electron density localized on the deprotonated amine nitrogen atom. This result suggests that FL1-NO formation occurs when NO attacks the deprotonated secondary amine of the coordinated ligand,

followed by inner-sphere electron transfer to Cu(II) to form Cu(I) and release of FL1-NO from the metal.

KEYWORDS: Biological signaling, nitric oxide, fluorescent sensor, mechanistic study.

Introduction

Nitric oxide (NO), once thought to be an environmental pollutant, is now recognized as an important biological signaling molecule that is responsible for cardiac function,¹⁻³ neurotransmission,⁴ and fighting invading pathogens during an immune response.⁵ Because of the radical character of NO its lifetime in solution under physiological conditions is limited,^{6,7} and nitrosated species such as *S*-nitrosothiols and *N*-nitrosamines are proposed to act as vehicles for nitric oxide storage and transport in biology.^{8,9} Transition metals are also major targets of NO attack, with the classic example being nitrosation of the heme iron of soluble guanylyl cyclase (sGC) to effect downstream vascular smooth muscle dilation.¹⁰ Nitric oxide can reductively nitrosylate metals, effecting one-electron reduction of the metal and nitros(yl)ation of a nucleophile by the resulting NO⁺ to form an E-NO species, where E is O, N or S.¹¹ This chemistry provides a mechanism by which small molecule metal complexes react with NO,¹¹⁻¹⁴ and it has also been employed as a strategy for nitric oxide sensing by transition metal-based sensors.¹⁵⁻²⁵

Recently, we reported one such NO-specific probe, CuFL1 (Fig. 1).^{19,20} The FL1 ligand is non-fluorescent, and DFT calculations revealed that quenching is due to photo-induced electron transfer from lone pair electrons delocalized throughout the aminoquinaldine unit into the half-filled fluorescein molecular orbital in the excited state.¹⁹ The fluorescence is further quenched by coordination to a paramagnetic Cu(II) ion. Treatment of a 1:1 mixture of FL1 and CuCl₂ in anaerobic buffered solutions with excess NO results in formation of a fluorescent species. Under similar anaerobic conditions, neither treatment of FL1 with NO nor addition of Cu(I) results in fluorescence enhancement. Upon exposure of CuFL1 to NO, the Cu(II) is reduced to Cu(I), as evidenced by optical, EPR, and UV-vis spectroscopy as well as ESI-MS studies, as well as the independent synthesis of FL1-NO.^{19,20} FL1-NO is emissive with a quantum yield of 0.58 ± 0.02 , compared to those of FL1 ($\phi = 0.077 \pm 0.002$) and CuFL1 ($\phi = 0.063 \pm$

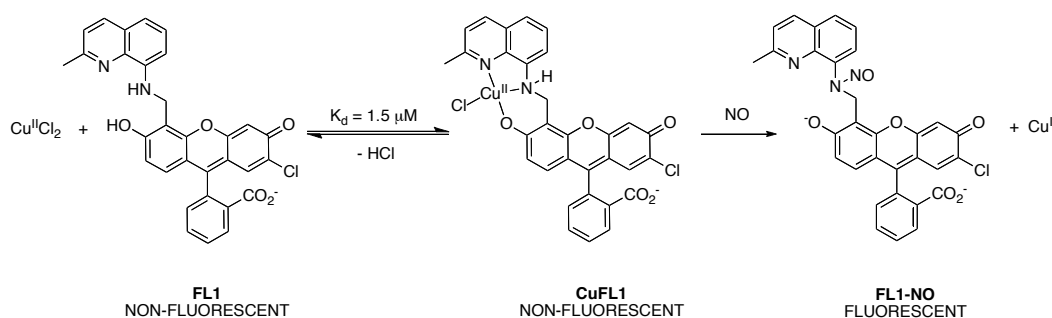
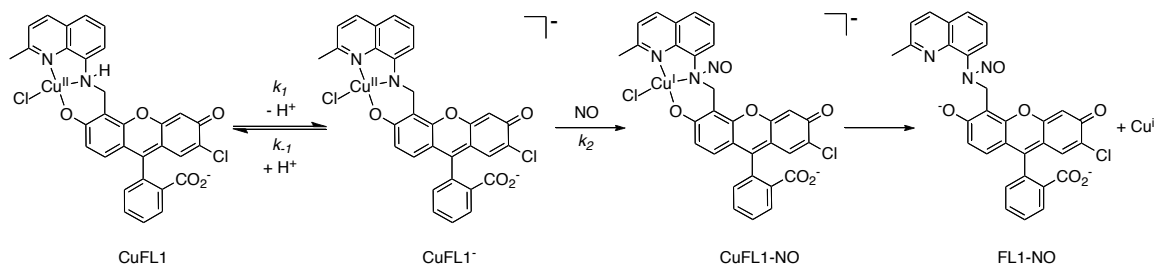


Figure 1. CuFL1 and its NO detection scheme.

0.002). Formation of FL1-NO with concomitant reduction of Cu(II) to Cu(I) is therefore responsible for the fluorescence enhancement observed when non-emissive CuFL1 reacts with NO (Fig. 1). Such an emission-enhancement mechanism is consistent with prior work²⁴ with a Cu(II) dianthracenyl cyclam complex, $[\text{Cu}(\text{DAC})]^{2+}$. A more detailed mechanistic examination of $[\text{Cu}(\text{DAC})]^{2+}$ suggested that NO reacts at a deprotonated secondary amine of the ligand with concomitant inner-sphere electron transfer to Cu(II) to produce Cu(I) and the nitrosated DAC-NO ligand as products.¹⁵

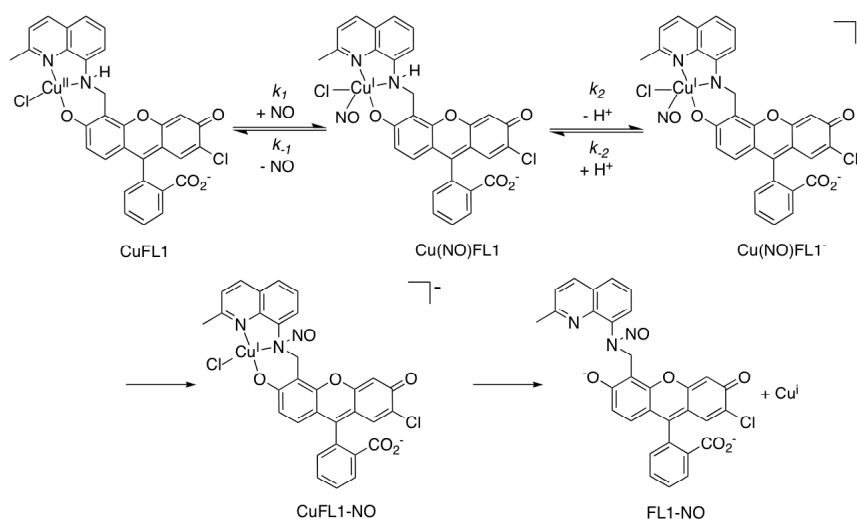
The reaction of CuFL1 with NO most likely proceeds through one of two possible intimate mechanisms. The first, mechanism 1, is analogous to that proposed for $[\text{Cu}(\text{DAC})]^{2+}$ and involves initial deprotonation of the secondary amine of the complexed ligand, followed by direct attack of NO at that site to form FL1-NO (Scheme 1), which would result in reduction of Cu(II) to Cu(I). The final step is release of the metal from FL1-NO, a poor ligand for the soft Cu(I) center owing to its hard oxygen and nitrogen donor atoms, inability to conform to tetrahedral geometry, and lowered electron density on the nitrosamine. The second, mechanism 2, invokes initial formation of a Cu(I)-NO complex (Scheme 2). Deprotonation of the secondary amine ligated to Cu(I)-NO would facilitate NO transfer from the metal to the ligand, again followed by release of Cu(I) from FL1-NO.

In the present article we present a kinetic and mechanistic investigation of the nitrosation of CuFL1 under varying conditions, including pH-dependent studies and an Eyring analysis, together with a spectroscopic evaluation of the electronic structure of CuFL1. These mechanistic tools have revealed the



Scheme 1. Proposed mechanism 1 for the reaction of CuFL1 with NO.

most likely preferred reaction pathway for the chemistry that underlies the turn-on fluorescence of the sensor.



Scheme 2. Proposed mechanism 2 for the reaction of CuFL1 with NO.

Experimental Section

Materials. 2-{2-Chloro-6-hydroxy-5-[(2-methylquinolin-8-ylamino)-methyl]-3-oxo-3*H*-xanthen-9-yl}benzoic acid (FL1) was prepared by a previously reported procedure.²⁰ All other chemicals were used as received. Piperazine-*N,N'*-bis(2-ethanesulfonic acid) (PIPES) was purchased from Calbiochem and potassium chloride (99.999%) was purchased from Aldrich. Buffer solutions (50 mM PIPES, 100 mM KCl, pH 6.0, 6.5, 7.0, 7.5, 8.0 and 8.7) were prepared in Millipore water and used for all spectroscopy except for pK_a titrations and solvent isotope effect determinations. pK_a titrations were performed in a solution of 20 mM KOH, 100 mM KCl, pH 12 in Millipore water. The pH of the solutions was adjusted

using 6, 1, or 0.1 N HCl and 0.1 N KOH. Potassium carbonate (Mallinckrodt) was used as a buffer for solvent isotope effect determinations. Buffer solutions (20 mM K₂CO₃, 100 mM KCl) were prepared at pH/D 7.0 in Millipore water or D₂O (Cambridge Isotope Laboratories), using a correction of 0.4 pH meter units to account for the differential readings of glass electrodes in D₂O.²⁶ For EPR experiments, solutions at pH 12.7 (50 mM KOH, 100 mM KCl), pH 10.1 (20 mM K₂CO₃, 100 mM KCl), pH 7.0 (50 mM PIPES, 100 mM KCl) and pH 4.0 (20 mM NaOAc, 100 mM KCl, sodium acetate purchased from Aldrich) were prepared in Millipore water. Copper chloride dihydrate (99+%) was purchased from Alfa Aesar and stock solutions of 10 mM and 1 mM were prepared in Millipore water. Stock solutions of 1 mM FL1 were prepared in DMSO and stored in aliquots at -80 °C.

Kinetic Studies of the Reaction of CuFL1 with Nitric Oxide. Absorbance measurements were made under anaerobic conditions, with cuvette solutions prepared in an inert atmosphere glove box. Buffer and CuCl₂ solutions were deoxygenated following standard procedures prior to use and stored under an inert atmosphere. Aliquots of FL1 were thawed immediately prior to use, deoxygenated using standard procedures, and brought under an inert atmosphere for sample preparation. Cuvette solutions were prepared by combining CuCl₂·2H₂O and FL1 in a 1:1 ratio in buffer and sealing the cuvette with a septum-equipped, gas-tight cap. Nitric oxide was purchased from Airgas and purified as previously described to minimize contamination by higher nitrogen oxides.²⁷ Nitric oxide gas was introduced into buffered solutions via gas-tight syringes. Samples were stirred throughout acquisitions to ensure equal distribution of NO throughout the sample solution. Acquisitions were made at 25.00 ± 0.05 °C unless otherwise noted. UV-vis spectra were acquired on a Cary 50-Bio spectrometer using spectrosil quartz cuvettes with gas-tight septa caps from Starna cells Inc. (3.5 mL volume, 1 cm path length). Measurements were recorded over 45 min using the scanning kinetics program in Cary WinUV v. 3.00, and changes in the intensity of the $\pi \rightarrow \pi^*$ transition of fluorescein at either 498 nm (decrease of CuFL1) or 504 nm (increase of FL1-NO) were monitored. The data were fit using OriginPro 8 software, and a regression analysis was performed using Microsoft Excel 2004, v. 11.5.6. All absorbance experiments

were performed in triplicate. Fluorescence spectra for pK_a titrations were obtained on a Quanta Master 4 L-format scanning spectrofluorimeter (Photon Technology International) at 25.0 ± 0.1 °C.

Electron Paramagnetic Resonance Measurements. EPR measurements were performed on a Bruker EMX EPR instrument at 9.33 GHz (X-band). EPR samples were prepared under anaerobic conditions in an inert atmosphere glove box. Stock solutions of 10 mM CuCl_2 and solutions of pH 12.7, 10.1, 7.0, and 4.0 were deoxygenated following standard procedures prior to use and stored under an inert atmosphere. Stock solutions of 5 mM FL1 were prepared in DMSO and stored in aliquots at -80 °C. Aliquots were thawed immediately prior to use, deoxygenated using standard procedures, and brought under an inert atmosphere for sample preparation. Samples were prepared by combining CuCl_2 and FL1 to final concentrations of 400 μM and 500 μM , respectively, such that 98.6% of Cu(II) was bound (determined from $K_d(\text{CuFL1}) = 1.5$ μM).^{19,20} Spectra were recorded as a frozen glass (8-10% DMSO in water). Spectra were reported from 4 scans with a time constant of 2.56 ms, modulation amplitude of 10 G, and microwave power of 2.01 mW. Samples were thawed, brought back under an inert atmosphere, and 500 μL of NO (g) was introduced to the samples via a gas-tight syringe. The samples were shaken to distribute NO throughout the solutions and then allowed to react at room temperature overnight (~ 13 h) in the dark. Samples were re-frozen into a glass prior to recording their post-NO treatment EPR spectra. Spectra were analyzed using the WINEPR System 2.11b.

Results and Discussion

Kinetic Studies of the Reaction of CuFL1 with NO. When anaerobic buffered solutions of CuFL1 were exposed to excess NO under pseudo-first-order conditions, the electronic spectra changed temporally in accord with expectations from previous work.²⁰ The CuFL1 band at 498 nm ($\pi \rightarrow \pi^*$ fluorescein transition) decreased slowly with concomitant growth of a new band at 504 nm corresponding to FL1-NO (Fig. 2). Well-anchored isosbestic points at 500 nm and 524 nm were observed, suggesting the formation of one spectroscopically observable product. A plot of the absorbance at 504 nm versus time revealed a rise in product formation (Fig. 2 inset), which fit well to a

first-order exponential eq (Fig. 2, inset), and such fittings were used to determine the observed rate constants (k_{obs}) for the reactions.

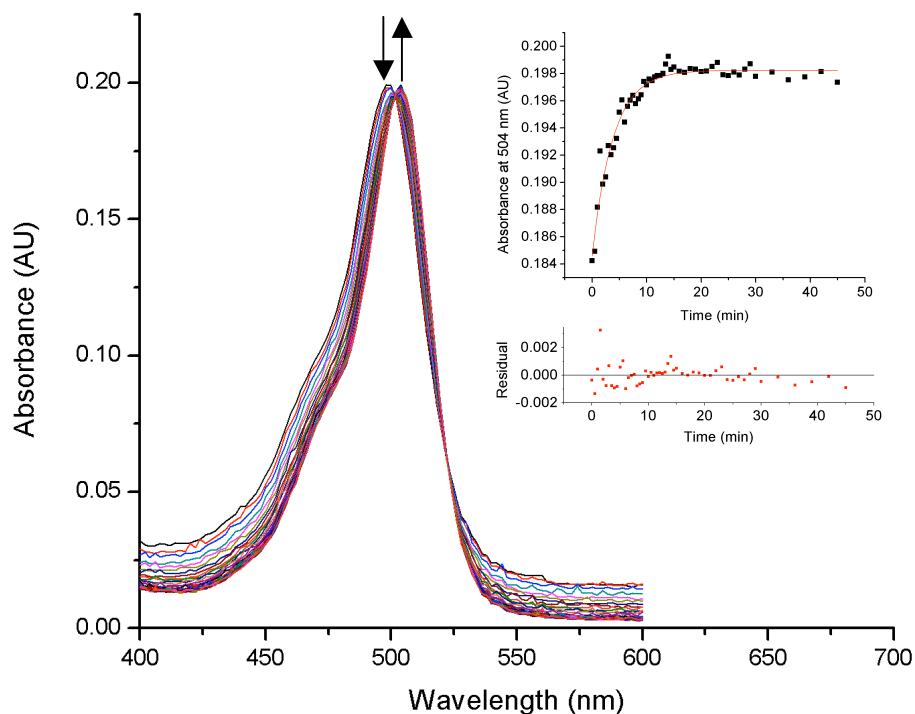


Figure 2. Plots of the absorbance vs. time for the reaction of 4 μM CuFL1 with 650 μM NO in 50 mM PIPES, 100 mM KCl, pH 7.0, T = 25 $^{\circ}\text{C}$. Inset: Absorbance at 504 nm vs. time (black dots) and the residuals from the exponential fit (red line).

Determining the Rate Equation for the Reaction of CuFL1 with NO. The rate of product formation was investigated as a function of changes in the concentrations of the reactants. Increases in [CuFL1],²⁸ [NO], and pH all accelerated the rate of FL1-NO formation. To determine the reaction order in [CuFL1], kinetic data were collected at constant pH, NO concentration, and temperature, and the concentration of CuFL1 was varied from 2 – 6 μM . A greater than 100-fold excess of NO (650 μM) was used to maintain pseudo-first-order conditions. The observed pseudo-first-order rate constants are summarized in Table 1, left-hand column. A plot of the k_{obs} values versus the concentration of CuFL1 revealed a linear relationship, and the corresponding log/log plot of k_{obs} versus [CuFL1] revealed a CuFL1 reaction order of unity (1.09 ± 0.09 after linear regression, Fig. 3). Although every effort was made to exclude dioxygen from the reaction, there is inadvertent O_2 leakage into the cuvettes over time,

Table 1. Kinetic Parameters for the Reaction of CuFL1 with NO.

[CuFL1] (μM) ^a	k_{obs} (s^{-1}) ^b	[NO] (μM) ^c	k_{obs} (s^{-1})	pH ^d	k_{obs} (s^{-1}) ^e
2	0.0022(5)	650	0.0040(3)	6.0	0.00068(6)
3	0.00324(9)	975	0.0046(6)	6.5	0.0017(2)
4	0.0040(3)	1300	0.008(2)	7.0	0.0039(3)
5	0.006(1)	1950	0.012(3)	7.5	0.008(2)
6	0.0072(9)	2600	0.014(4)	8.0	0.011(4)
				8.7	0.014(6)

^a Measurements were performed in 50 mM PIPES, 100 mM KCl, pH 7.0, T = 25 °C, [NO] = 650 μM .

^b k_{obs} values were determined by fitting the absorbance at 504 nm versus time to a single exponential equation, $y = Ae^{(-x/t)} + y_0$

^c Measurements were performed in 50 mM PIPES, 100 mM KCl, pH 7.0, T = 25 °C, [CuFL1] = 4 μM . ^d Measurements were performed in 50 mM PIPES, 100 mM KCl, T = 25 °C, [CuFL1] = 4 μM , [NO] = 650 μM . ^e k_{obs} values were determined by fitting the absorbance at 498 nm for pH 6.0 and 6.5.

which differentially affects the reactions based on their rate. Therefore, the most likely source of error in the measurements is the NO concentration, which varies if dioxygen is present due to the formation of higher nitrogen oxides. Despite this systematic error, the slope of the log-log plot clearly indicates a first-order dependence on the concentration of CuFL1.

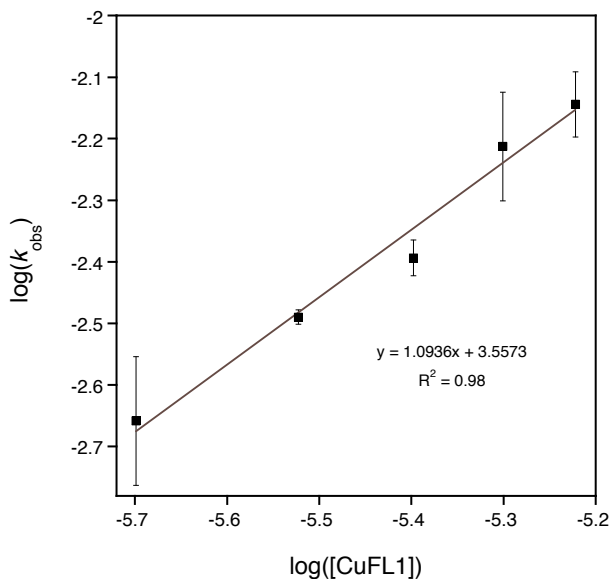


Figure 3. Plot of the $\log(k_{\text{obs}})$ vs. the $\log([\text{CuFL1}])$ for the reactions of 2 – 6 μM CuFL1 with 650 μM NO in 50 mM PIPES, 100 mM KCl, pH 7.0, T = 25 °C.

To determine the reaction order in NO concentration, kinetic data were collected at constant pH, CuFL1 concentration, and temperature (Table 1, middle column). Again, a greater than 100-fold excess

of NO was used (650 μM NO vs. 4 μM CuFL1 for the lowest [NO]). The highest NO concentration used, 2.6 mM, was at the supersaturation point,²⁹ and the error for the k_{obs} values therefore increased with the NO concentration. However, a plot of the k_{obs} values versus NO concentration still revealed a linear relationship, as did the corresponding log/log plot of k_{obs} versus [NO] (Fig. 4). The slope of the latter revealed a first-order dependence of the reaction on the concentration of NO (1.0 ± 0.1 after linear regression analysis).

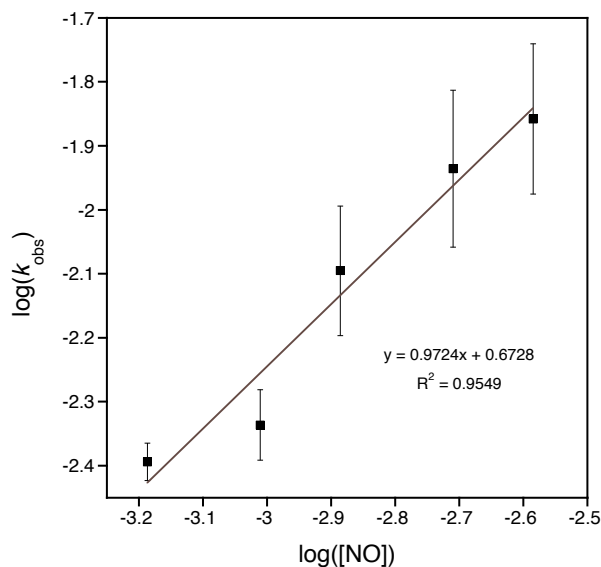


Figure 4. Plot of the $\log(k_{\text{obs}})$ vs. the $\log([\text{NO}])$ for the reactions of 4 μM CuFL1 with 650 - 2600 μM NO in 50 mM PIPES, 100 mM KCl, pH 7.0, $T = 25\text{ }^\circ\text{C}$.

To determine the order of the reaction in $[\text{OH}^-]$, kinetic data were collected at constant NO (650 μM) and CuFL1 (4 μM) concentrations and constant temperature (Table 1, right-hand column). The obtained k_{obs} values revealed a more complex pH dependence than was observed for the NO or CuFL1 concentrations. The rate constants increased with increasing pH, which is consistent with the hypothesis that deprotonation of the secondary amine of FL1 is required for reaction of CuFL1 with NO. A plot of the k_{obs} values versus $[\text{OH}^-]$ revealed saturation behavior at high $[\text{OH}^-]$ (Fig. 5a). The plot of the k_{obs} values versus pH (Fig. 5b) illustrates that, below pH 7, the observed rate constants also begin to plateau, again consistent with the hypothesis that protonation state of the complex is crucial to progress of the reaction and formation of the *N*-nitrosated product. These data also provide important information

informing the design of new NO-specific Cu(II)-based probes. In particular, it is clear that by lowering the pK_a of the complexed secondary amine it would be possible to increase the rate of the reaction with NO. This feature could be valuable for biological NO sensing, because NO is highly reactive with many physiological components such as amines, thiols, oxygen and metal centers owing to its radical character. Increasing the rate of its reaction with CuFL1 and related sensors would assure the utility of the probe for biological experimentation for where fast temporal resolution is required.

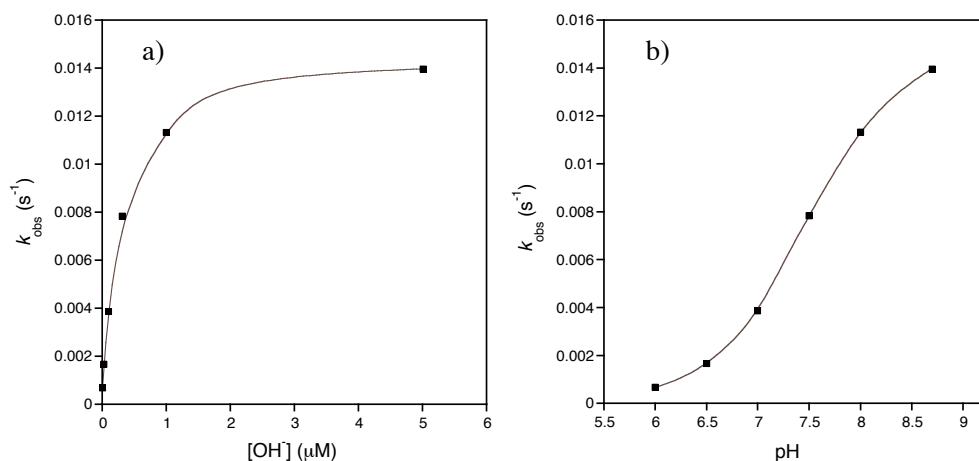


Figure 5. a) Plot of the k_{obs} vs. $[OH^-]$ for the reactions of 4 μM CuFL1 with 650 μM NO in 50 mM PIPES, 100 mM KCl, pH 6.0 – 8.7, T = 25 °C. b) Plot of the k_{obs} vs. pH.

pH Titrations of FL1 and CuFL1. Because of the importance of secondary amine deprotonation in the reaction of CuFL1 with NO, the pK_a values of the both FL1 and the CuFL1 complex were determined. Spectral changes of FL1 at different pH values were monitored by UV-vis and fluorescence spectroscopy and displayed behavior that is typical for fluorescein-based ligands (Fig. 6). The absorbance data (Fig. 6a) could be fit to obtain a $pK_{a(UV)}$ value of 5.6. The fluorescence data (Fig. 6b) revealed three pK_a values of 4.7 ($pK_{a(FLuor1)}$, Fig. S1a), 5.6 ($pK_{a(FLuor2)}$), and 6.5 ($pK_{a(FLuor3)}$, Fig. S1b). The $pK_{a(FLuor3)}$ value agrees well with the pK_a value of 6.1 determined by fluorescence for a related Zn(II) sensor, QZ1,³⁰ which was assigned to the secondary amine nitrogen atom. The $pK_{a(FLuor1)}$ value of 4.7 probably corresponds to a combination of fluorescein carboxylic acid protonation ($pK_a = 4.4$ for fluorescein, 3.5 for dichlorofluorescein)^{31,32} and lactonization of the fluorescein. The intermediate $pK_{a(FLuor2)}$ value of 5.6 can be assigned to the quinaldine nitrogen atom (5.08 ± 0.5 for *N*,2-dimethyl-8-

quinolinamine).³³ The UV-vis data are not sufficiently well resolved to determine all three pK_a values, allowing only computation of an apparent pK_a ($pK_{a(UV)}$). The average of all three fluorescence pK_a values of 5.6 is consistent with the $pK_{a(UV)}$ value.

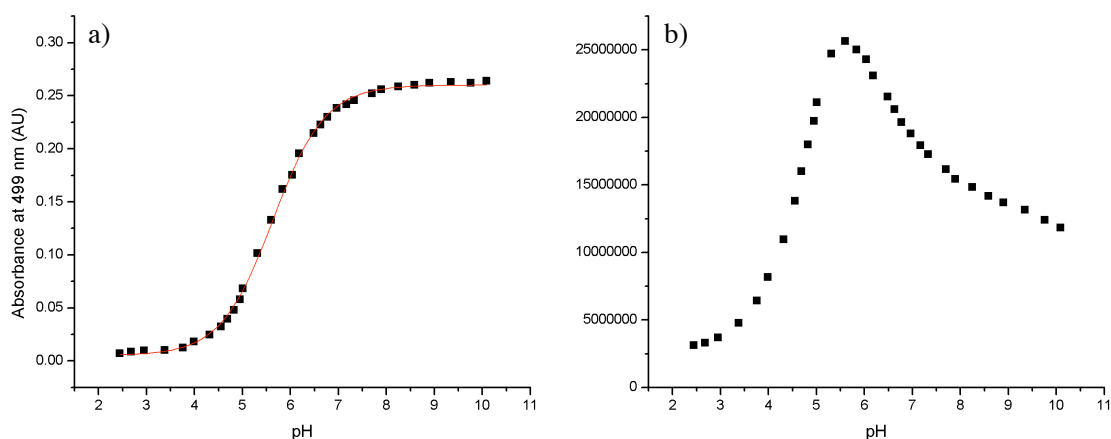


Figure 6. a) Absorbance dependence on pH, with fit, for 5 μ M FL1 in 20 mM KOH, 100 mM KCl, pH \sim 12, T = 25 $^{\circ}$ C. pH adjusted with 6 N, 1 N and 0.1 N HCl and 0.1 N KOH. b) Fluorescence emission dependence on pH. pK_a values were determined by fitting the plots of absorbance or integrated fluorescence emission at λ_{max} vs. pH to the equation, $y = (A_1 - A_2)/(1 + e^{(x-pK_a)/dx}) + A_2$.

When the same experiment was repeated for CuFL1, the fluorescence data again revealed three pK_a values in the region of pH 2.5 – 9, and a fourth value above 9 that could not be adequately resolved (Fig. 7a). The fluorescence data from pH 2.5 – 6.5 were fit to obtain the first value ($pK_{a(FLuor1)}$) of 4.9 (Fig. S2a), the maximum revealed the second value ($pK_{a(FLuor2)}$) of 6.4, and the third value ($pK_{a(FLuor3)}$) of 7.7 was obtained by fitting the fluorescence data from pH 6.5 – 9 (Fig. S2b). The UV-vis data for CuFL1, however, differed from those of FL1 in that two pK_a values were obtained (Fig. 7b). Fits of the data from pH 2.5 – 5.5 (Fig. S3a) and from 6 – 11 (Fig. S3b) revealed values of 4.7 and 7.5 for $pK_{a(UV1)}$ and $pK_{a(UV2)}$, respectively. These results are in good agreement with those obtained from the fluorescence data and most likely correspond to the pK_a value for deprotonation of the secondary amine ligated to Cu(II) (7.7 and 7.5) and the pK_a value of the fluorescein bottom-ring carboxylic acid/lactonization of the fluorescein (4.9 and 4.7). The absence of a third, intermediate pK_a value in the absorbance data confirms the assignment that it belongs to the quinoline nitrogen atom, which would be bound to Cu(II) in the complex and therefore not protonated.

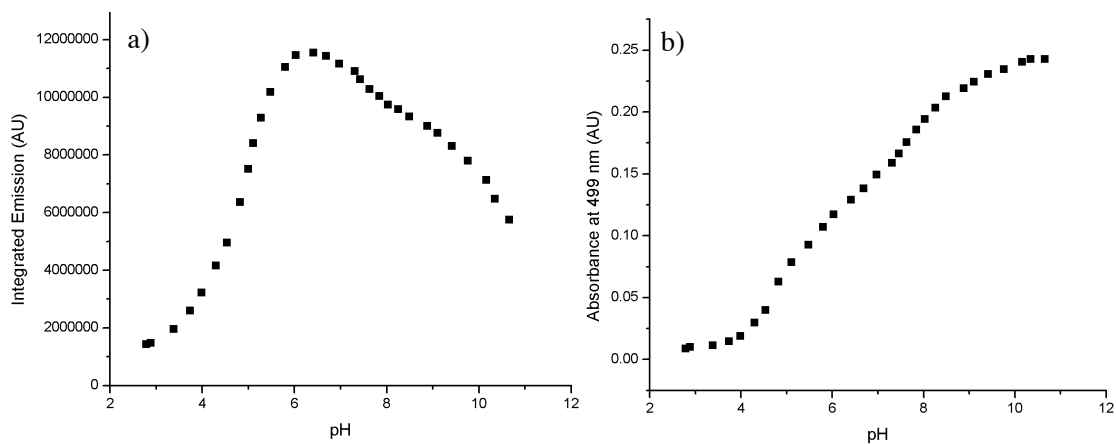


Figure 7. a) Fluorescence emission dependence on pH for 5 μM CuFL1 in 20 mM KOH, 100 mM KCl, pH \sim 12, T = 25 $^{\circ}\text{C}$. pH adjusted with 6 N, 1 N and 0.1 N HCl and 0.1 N KOH. b) Absorbance dependence on pH.

Activation Parameters of the Reaction of CuFL1 with NO. An Eyring analysis was performed to determine the activation parameters associated with the reaction of CuFL1 with NO. Kinetic runs were performed over a temperature range of 5 – 40 $^{\circ}\text{C}$, and the k_{obs} values obtained were plotted as the natural logarithm of k_{obs}/T versus $1/T$ to obtain the enthalpy and entropy of activation, ΔH^{\ddagger} and ΔS^{\ddagger} , respectively (Fig. 8 and Table 2). The activation energy (E_a) was determined from a plot of the natural logarithm of k_{obs} versus $1/T$. The enthalpy of activation ($\Delta H^{\ddagger} = 9.7 \pm 0.5$ kcal/mol) and activation energy ($E_a = 10.3 \pm 0.5$ kcal/mol) indicate a relatively low activation barrier for the reaction and are consistent with values obtained from other experimental and theoretical examinations of nitrosation of secondary amines.³⁴⁻³⁶ The negative entropy of activation ($\Delta S^{\ddagger} = -29 \pm 3$ cal/mol·K) is consistent with an associative nitrosation mechanism.

Table 2. Activation Parameters for the Reaction of CuFL1 with NO.

T (K)	k_{obs} (s^{-1}) ^{a, b}	E_a (kcal/mol) ^c
278.15	0.0011(2)	10.3(5)
288.15	0.0019(8)	ΔH^{\ddagger} (kcal/mol) ^d
298.15	0.0041(2)	9.7(5)
308.15	0.0061(6)	ΔS^{\ddagger} (cal/mol·K) ^d
313.15	0.008(2)	-29(3)

^a Measurements were performed in 50 mM PIPES, 100 mM KCl, pH 7.0, T = 278.15 – 313.15 K, [CuFL1] = 4 μM , [NO] = 650 μM . ^b k_{obs} values were determined by fitting the plot of absorbance at 504 nm versus time to a single exponential equation, $y = Ae^{(-x/t)} + y_0$. ^c $k_{\text{obs}} = Ae^{-(E_a/RT)}$. ^d $k_{\text{obs}} = (k_B T/h)\exp(\Delta S^{\ddagger}R)\exp(-\Delta H^{\ddagger}/RT)$.

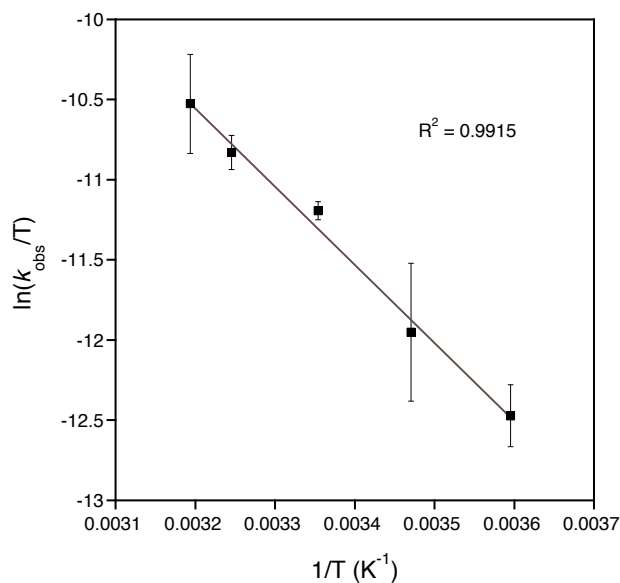


Figure 8. Eyring plot for the reaction of 4 μM CuFL1 with 650 μM NO in 50 mM PIPES, 100 mM KCl, pH 7.0, T = 278.15 – 313.15 K.

pH-Dependent EPR Spectroscopy of CuFL1. EPR spectra were recorded at four pH values to determine whether the protonation state of the secondary amine affects the distribution of the unpaired electron spin density (Fig. 9). At pH 4.0 the secondary amine ($pK_a \sim 7.5$) should be fully protonated, and the observed EPR spectrum is typical of that for a rhombically distorted axial Cu(II) species with $g_{\parallel} = 2.36$, $g_{\perp} = 2.08$, and $A_{\parallel}(\text{Cu}) = 463$ MHz (Fig. 9a). The perpendicular hyperfine coupling constant is smaller than the peak width of the perpendicular signal component and therefore cannot be determined. When the pH is increased to 7.0, the spectrum loses resolution, but still retains axial Cu(II) character with hyperfine features. The approximate g values are $g_{\parallel} = 2.39$ and $g_{\perp} = 2.08$ and the Cu(II) hyperfine coupling constant $A_{\parallel}(\text{Cu})$ is ~ 529 MHz (Fig. 9b). It is possible that broadening at pH 7.0 is observed because there is a mixture of CuFL1 and CuFL1⁻, where CuFL1⁻ is the complex in which the secondary amine has been deprotonated (see Scheme 1). At pH 10.1, however, two distinct Cu(II)-based spin active species are observed (Fig. 9c). At this pH the Cu(II)-amido species, CuFL1⁻, should be fully populated, that is, the ligand should be fully deprotonated ($pK_a \sim 7.5$). The two observed species could be water- and hydroxide-bound Cu(II) complexes. The Cu(II)-amido species probably has both Cu(II)-radical and nitrogen-centered radical character. The latter may result in the decreased separation of g_{\parallel}

and g_z observed, because N -centered radicals tend to be more isotropic than Cu(II) complexes, with g values that lie closer to that of the free electron ($g = 2.0023$). Finally, at pH 12.7, ^{14}N hyperfine coupling from the N -centered radical appears to be present in the spectrum, and the Cu(II)-based species are poorly resolved (Fig. 9d). Although a definitive assignment of the multi-line splitting pattern resulting from significant $A(^{14}\text{N})$ contribution is difficult, the spectrum displays features similar to those reported for a Cu(I)-aminyl radical species.³⁷ A nitrogen-centered radical would be an excellent target for attack by NO.

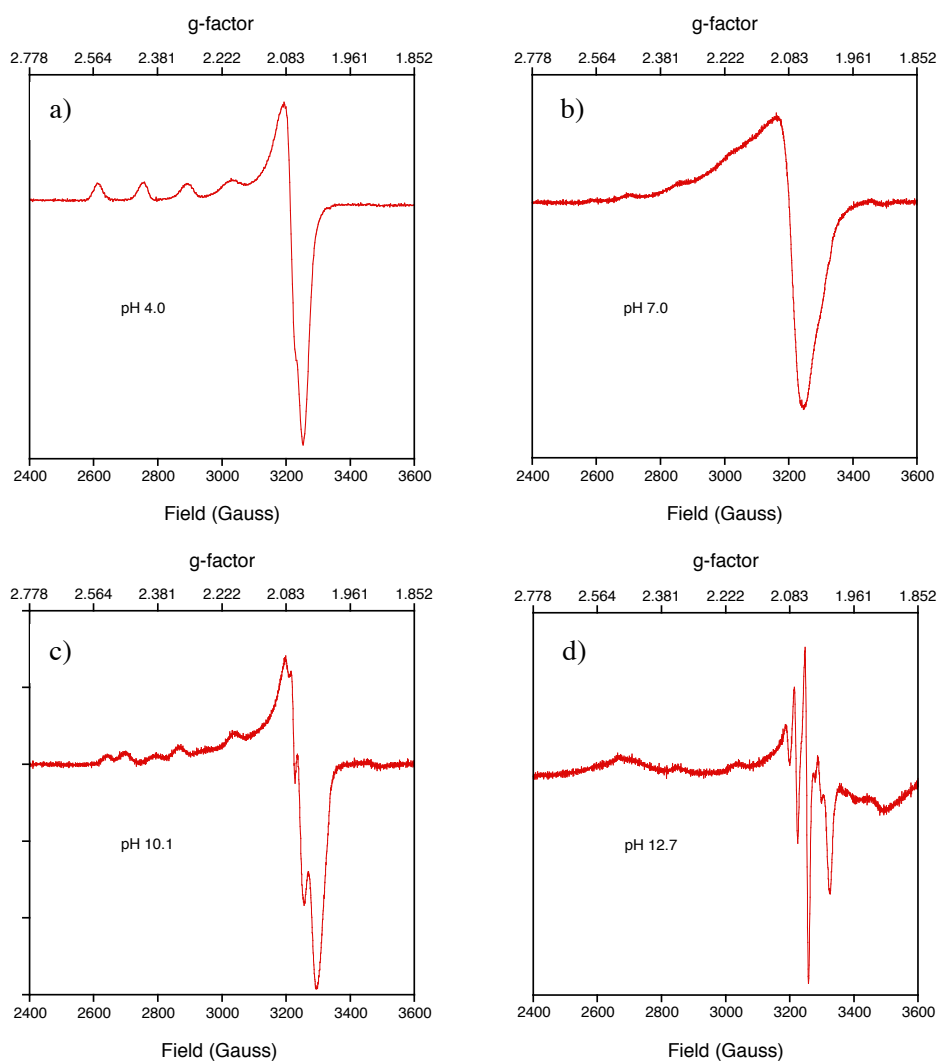


Figure 9. EPR spectra of CuFL1 at a) pH 4.0, b) pH 7.0, c) pH 10.1, and d) pH 12.7.

If a copper-nitrosyl adduct were formed during the reaction of CuFL1 with NO via mechanism 2 (vide supra), it probably could be detected by EPR spectroscopy under conditions where the secondary amine nitrogen remains protonated. To evaluate this possibility, nitric oxide was introduced anaerobically to a solution of CuFL1 in pH 4.0 buffer in an EPR tube, which was shaken and allowed to stand at room temperature for 13 h. The sample was then frozen and the EPR spectrum was recorded using conditions identical to those employed to record the spectrum prior to the introduction of NO. If a CuFL1-NO adduct were formed it would be diamagnetic, and consequently reduction of the Cu(II)-based signal intensity would be expected. The corresponding spectra, which are depicted in Fig. S4, show no changes in the EPR signal before or after NO addition, suggesting that there is no copper-nitrosyl formation under these conditions.

Effects of Isotopic Substitution on k_{obs} . Given the pH dependence of the spectral properties of FL1 and CuFL1 and the observation that deprotonation of the secondary amine facilitates reaction with NO, the effect of isotopic substitution (D for H) at the secondary amine nitrogen atom was investigated to determine whether the rate-limiting step might involve deprotonation at this site. Kinetic runs were performed under pseudo-first-order conditions (650 μM NO, > 100-fold excess) at a fixed concentration of 4 μM CuFL1 at 25.0 $^{\circ}\text{C}$ in either H_2O or D_2O at pH/D 7.0.²⁶ Plots of the absorbance at 500 nm versus time were fit to first-order exponential equations in order to determine the observed rate constants (k_{obs}), which were then compared to extract the solvent isotope effect ($\text{SIE} = k_{\text{obs}}(\text{H})/k_{\text{obs}}(\text{D})$). The average $k_{\text{obs}}(\text{H})$ of $0.23 \pm 0.2 \text{ min}^{-1}$ over $k_{\text{obs}}(\text{D})$ of $0.11 \pm 0.01 \text{ min}^{-1}$ gave an SIE of 2.0 ± 0.3 , consistent with the hypothesis that deprotonation of the secondary amine nitrogen atom is an important mechanistic step. Although normally an SIE of 2 would suggest that proton-transfer occurs in the rate-determining step, the case of CuFL1 is more complicated because the $\text{p}K_{\text{a}}$ of the complexed amine ($\text{p}K_{\text{a}} \sim 7.5$) will change with D substitution; substitution of N–H by N–D alters the acid-base equilibrium of the initial complex. Therefore, in addition to the decreased rate that might be expected because of isotopic substitution based on N–H/D bond breaking, the reaction rate might also be reduced because the deuterated secondary amine is at a different point in its acid-base equilibrium at pH 7.0 compared to the undeuterated

secondary amine. Because CuFL1 is only reactive with NO in protic solvents, the kinetic and solvent isotope effects could not be separated by using an aprotic solvent such as acetonitrile. Therefore, although the SIE suggests that proton-transfer occurs in the rate-determining step, the complicating factor of the acid-base equilibrium makes it difficult to draw a definitive conclusion based on this experiment alone.

Mechanistic Insights. Based on the kinetic data and activation parameters, the hypotheses for the mechanism of the reaction of CuFL1 with NO can now be examined. The first mechanism invoked an initial deprotonation step, followed by reaction of NO at the deprotonated secondary amine with concomitant reduction of Cu(II) to Cu(I) via an inner-sphere electron transfer (Scheme 1). If deprotonation were rate limiting, then the rate law would be given by eq 1. Because the kinetic data revealed the reaction to be first order in [NO], mechanism 1, in the case of rate-limiting deprotonation,

$$\text{rate} = k_1[\text{CuFL1}][\text{OH}^-] \quad (1)$$

can be excluded. If, however, reaction of the deprotonated complex with NO were rate limiting, i.e. there is a fast pre-equilibrium between the protonated and deprotonated CuFL1, then the rate law becomes that given by eq 2. The [CuFL1⁻] can be determined from the acid-base equilibrium as defined

$$\text{rate} = k_2[\text{CuFL1}^-][\text{NO}] \quad (2)$$

$$K_{\text{eq}} = \frac{[\text{CuFL1}^-][\text{H}^+]}{[\text{CuFL1}]} \quad (3)$$

$$\text{rate} = \frac{k_2 K_{\text{eq}} [\text{CuFL1}][\text{NO}]}{[\text{H}^+]} \quad (4)$$

in eq 3. Rearranging eq 3 and substituting into eq 2 yields the rate law shown in eq 4 when reaction with NO is rate-limiting. This rate law is consistent with the concentration dependence results. At high pH, rate saturation was observed, and under these circumstances the rate law should not depend on [H⁺]. If

mechanism 1 were operative at high pH, the rate would be limited by reaction with NO and would be described by eq 5, which is also consistent with the results of the concentration dependence experiments. Therefore, mechanism 1 is viable if reaction with NO is rate limiting, and it also applies at high pH.

$$\text{rate} = k_2[\text{CuFL1}^-][\text{NO}] = k_2[\text{CuFL1}][\text{NO}] \quad (5)$$

The second mechanism involves an initial, reversible reaction of CuFL1 with NO to form a Cu(I)-NO⁺ species, followed by deprotonation of the secondary amine and subsequent fast translocation of NO⁺ to form the *N*-nitrosated ligand with release of Cu(I) (Scheme 2). If reaction with NO were rate limiting, then the rate law given by eq 6. Because the reaction is pH dependent, mechanism 2 cannot be

$$\text{rate} = k_1[\text{CuFL1}][\text{NO}] \quad (6)$$

operative in the case of rate-limiting reaction with NO. If instead deprotonation of Cu(NO)FL1 were rate-limiting, then the rate law is given by that shown in eq 7, which cannot be solved analytically but is

$$\text{rate} = \left(\frac{k_2[\text{OH}^-]}{k_{-1} + k_2[\text{OH}^-]} \right) (k_1[\text{CuFL1}][\text{NO}] + k_{-2}[\text{Cu(NO)FL}^-][\text{H}^+]) \quad (7)$$

dependent on all the reactants. If mechanism 2 were operative at high pH, the rate law would again be described by eq 5, consistent with the experimental data. Therefore, mechanism 2 is a viable mechanism if deprotonation is rate-limiting, and it would certainly apply at high pH.

One can also envision alternative mechanisms involving outer sphere electron transfer between the Cu(II) center and NO to form Cu(I)FL1 and NO⁺ followed by steps from either mechanisms 1 or 2. In either of these cases, however, the reaction order in NO concentration would most likely be >1, owing to scavenging of NO⁺ by H₂O, which can be ruled out by the data.

The pH titrations support the hypothesis that, at high pH, the reaction with NO is rate-limiting and the rate ceases to depend on [OH⁻]. Saturation kinetics are therefore expected at pH values above the pK_a

value of the Cu(II)-bound secondary amine ($pK_a \sim 7.5$), which is consistent with the observed data. The rates begin to plateau at $pH \sim 8$, but do not fully saturate until after at least $pH 8.7$, more than 1 pH unit above the pK_a . The activation parameters are also consistent with both mechanisms 1 and 2. The activation entropy indicates an associative rate-limiting step, which can be envisioned for either mechanism, with NO and CuFL1 coming together in the transition state.

The two hypothesized mechanisms – either an initial deprotonation followed by attack of NO at the secondary amine (mechanism 1) or formation of a Cu-NO species followed by deprotonation and NO^+ migration to the ligand (mechanism 2) – are indistinguishable at neutral pH or below, except for the rate-limiting step. For mechanism 1 to be valid, reaction with NO must be rate-limiting, whereas for mechanism 2 to be valid, deprotonation must be rate-limiting. The solvent isotope effect experiments indicate that deprotonation of the secondary amine of the complexed ligand is important in the reaction mechanism. However, because the magnitude of the SIE cannot be determined accurately under these conditions (*vide supra*), no insights into the rate-limiting step of the reaction are provided by these data.

According to DFT calculations on the reaction of nitric oxide with $[Cu(DAC)]^{2+}$, formation of a Cu(II)-NO complex is entropically disfavored and the binding is predicted to be weak.¹⁵ On the basis of this finding and the fact that no Cu-NO stretch could be observed in an IR experiment in which $[Cu(DAC)]Br_2$ was allowed to react with NO under conditions where deprotonation of $[Cu(DAC)]^{2+}$ would not be expected, mechanism 1 was deemed to be more plausible. Because of the limited solubility of CuFL1 in acetonitrile, the analogous IR experiment could not be performed in the current system; however, EPR data from the reaction of CuFL1 and NO at $pH 4.0$ (*vide supra*) similarly indicate lack of Cu-NO adduct formation at low pH. The absence of evidence for a Cu(I)-NO species under conditions favoring proton retention of the secondary amine in FL1 does not exclude the possibility either that a Cu(I)-NO adduct can be formed at higher pH or that a Cu(I)-NO species is too short-lived to accumulate to an appreciable steady-state concentration under these conditions. We therefore do not discount formation of a Cu(I)-NO adduct as a mechanistic intermediate. The fact that the EPR spectrum changes from that of an axial Cu(II) signal at $pH 4.0$ to what appears to be a mixed Cu(II)-based/*N*-

based signal at pH 12.7 suggests that, as CuFL1 is deprotonated, an *N*-centered radical species is formed. Such formally Cu(I)-aminyl species would provide a site on the ligand for NO attack. Because Cu(I)–nitrosyls are generally considered to be unstable,³⁸⁻⁴⁰ we conclude that the reaction of CuFL1 with NO most likely proceeds by a mechanism that does not require formation of such an unstable species. Instead, we favor mechanism 1 as the preferred route.

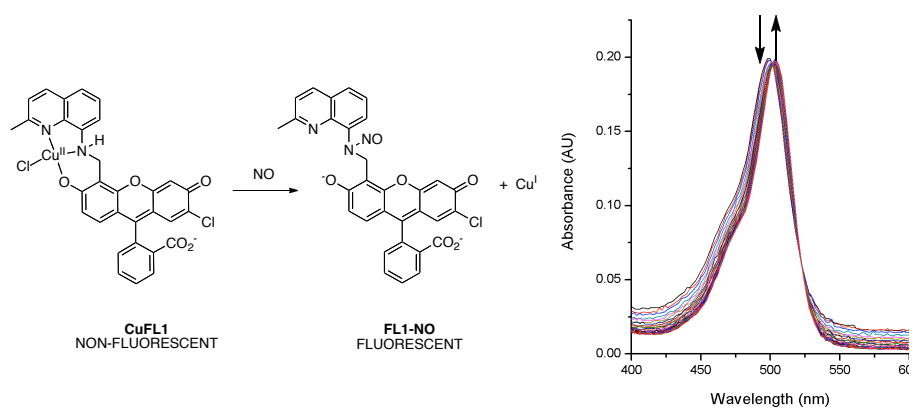
Summary

The reaction of CuFL1 with NO in aqueous, buffered solutions is first order in the concentration of CuFL1 and NO and also depends on the hydroxide ion concentration. Saturation kinetics occur at high base concentrations, which is consistent with deprotonation of the secondary amine of CuFL1 as a key mechanistic step. These results predict that a CuFL1-type probe with a lower secondary amine pK_a would result in a superior NO detector for *in vivo* applications. The activation parameters indicate an associative reaction. EPR experiments at various pH values suggest that, as CuFL1 is deprotonated, the unpaired electron density shifts from copper to nitrogen, yielding new spin-active species. Two mechanistic interpretations fit the data, with one that invokes initial deprotonation of bound FL1 at the secondary amine followed by direct attack of NO at the deprotonated ligand being most likely.

Acknowledgement. This work was supported by grant CHE-0907905 from the National Science Foundation (NSF). M.D.P. thanks the NIH for postdoctoral fellowships (5 F32 GM085930 and 1 K99 GM092970). Spectroscopic instrumentation at the MIT Department of Chemistry Instrument Facility is maintained with funding from the National Institutes of Health (NIH) grant NIH 1S10RR003850-01. We thank Drs. Zachary Tonzitech and Neal Mankad for insightful discussions. The content is solely the responsibility of the authors and does not necessarily represent the official views of the National Institute of General Medical Sciences or the National Institutes of Health.

Supporting Information Available: Fits of pH titrations of FL1 and CuFL1; EPR spectra before and after NO addition at pH 4.0. This material is available free of charge via the Internet at <http://pubs.acs.org>

TOC GRAPHIC:



References

1. Furchgott, R. F.; Vanhoutte, P. M. *FASEB J.* **1989**, *3*, 2007-2018.
2. Ignarro, L. J.; Buga, G. M.; Wood, K. S.; Byrns, R. E.; Chaudhuri, G. *Proc. Natl. Acad. Sci. U. S. A.* **1987**, *84*, 9265-9269.
3. Rapoport, R. M.; Draznin, M. B.; Murad, F. *Nature* **1983**, *306*, 174-176.
4. Garthwaite, J. *Eur. J. Neurosci.* **2008**, *27*, 2783-2802.
5. Bogdan, C. *Nat. Immunol.* **2001**, *2*, 907-916.
6. Liu, X.; Miller, M. J. S.; Joshi, M. S.; Thomas, D. D.; Lancaster, J. R., Jr. *Proc. Natl. Acad. Sci. U. S. A.* **1998**, *95*, 2175-2179.
7. Thomas, D. D.; Liu, X.; Kantrow, S. P.; Lancaster, J. R., Jr. *Proc. Natl. Acad. Sci. U. S. A.* **2001**, *98*, 355-360.
8. Gladwin, M. T.; Schechter, A. N. *Circ. Res.* **2004**, *94*, 851-855.
9. Vanin, A. F. *Biochemistry (Moscow, Russ. Fed.)* **1998**, *63*, 782-793.
10. Cary, S. P. L.; Winger, J. A.; Derbyshire, E. R.; Marletta, M. A. *Trends Biochem. Sci.* **2006**, *31*, 231-239.
11. Ford, P. C.; Fernandez, B. O.; Lim, M. D. *Chem. Rev.* **2005**, *105*, 2439-2455, and refs. cited therein.
12. Melzer, M. M.; Mossin, S.; Dai, X.; Bartell, A. M.; Kapoor, P.; Meyer, K.; Warren, T. H. *Angew. Chemie. Int. Ed.* **2010**, *49*, 904-907.
13. Sarma, M.; Singh, A.; Gupta, G. S.; Das, G.; Mondal, B. *Inorg. Chim. Acta* **2010**, *363*, 63-70.
14. Tran, D.; Skelton, B. W.; White, A. H.; Laverman, L. E.; Ford, P. C. *Inorg. Chem.* **1998**, *37*, 2505-2511.
15. Khin, C.; Lim, M. D.; Tsuge, K.; Iretskii, A.; Wu, G.; Ford, P. C. *Inorg. Chem.* **2007**, *46*, 9323-9331.
16. Lim, M. H.; Lippard, S. J. *J. Am. Chem. Soc.* **2005**, *127*, 12170-12171.
17. Lim, M. H.; Lippard, S. J. *Inorg. Chem.* **2006**, *45*, 8980-8989.
18. Lim, M. H.; Lippard, S. J. *Acc. Chem. Res.* **2007**, *40*, 41-51.
19. Lim, M. H.; Wong, B. A.; Pitcock, W. H., Jr.; Mokshagundam, D.; Baik, M.-H.; Lippard, S. J. *J. Am. Chem. Soc.* **2006**, *128*, 14364-14373.
20. Lim, M. H.; Xu, D.; Lippard, S. J. *Nat. Chem. Biol.* **2006**, *2*, 375-380.
21. Ouyang, J.; Hong, H.; Shen, C.; Zhao, Y.; Ouyang, C.; Dong, L.; Zhu, J.; Guo, Z.; Zeng, K.; Chen, J.; Zhang, C.; Zhang, J. *Free Radical Biol. Med.* **2008**, *45*, 1426-1436.
22. Smith, R. C.; Tennyson, A. G.; Lim, M. H.; Lippard, S. J. *Org. Lett.* **2005**, *7*, 3573-3575.
23. Smith, R. C.; Tennyson, A. G.; Won, A. C.; Lippard, S. J. *Inorg. Chem.* **2006**, *45*, 9367-9373.
24. Tsuge, K.; DeRosa, F.; Lim, M. D.; Ford, P. C. *J. Am. Chem. Soc.* **2004**, *126*, 6564-6565.
25. Xing, C.; Yu, M.; Wang, S.; Shi, Z.; Li, Y.; Zhu, D. *Macromol. Rapid Commun.* **2007**, *28*, 241-245.
26. Glasoe, P. K.; Long, F. A. *J. Phys. Chem.* **1960**, *64*, 188-190.
27. Lim, M. D.; Lorkovic, I. M.; Ford, P. C. *Methods Enzymol.* **2005**, *396*, 3-17.
28. $[\text{CuFL1}] = [\text{Cu(II)}] = [\text{FL1}]$, and assumes no dissociation of Cu(II) from the complex.
29. Shaw, A. W.; Vosper, A. J. *J. Chem. Soc. Faraday Trans.* **1977**, *73*, 1239-1244.
30. Nolan, E. M.; Jaworski, J.; Okamoto, K.-I.; Hayashi, Y.; Sheng, M.; Lippard, S. J. *J. Am. Chem. Soc.* **2005**, *127*, 16812-16823.
31. Diehl, H.; Horchak-Morris, N. *Talanta* **1987**, *34*, 739-741.
32. Leonhardt, H.; Gordon, L.; Livingston, R. *J. Phys. Chem.* **1971**, *75*, 245-249.
33. Calculated using Advanced Chemistry Development (ACD/Labs) Software V8.14 (© 1994-2010 ACD/Labs).
34. Casado, J.; Castro, A.; Leis, R. R.; López Quintela, M. A.; Mosquera, M. *Monatsh. Chem.* **1983**, *114*, 639-646.

35. González-Mancebo, S.; Calle, E.; García-Santos, M. P.; Casado, J. *J. Agric. Food Chem.* **1997**, *45*, 334-336.
36. Zhao, Y.-L.; Garrison, S. L.; Gonzalez, C.; Thweatt, W. D.; Marquez, M. *J. Phys. Chem. A* **2007**, *111*, 2200-2205.
37. Mankad, N. P.; Antholine, W. E.; Szilagyi, R. K.; Peters, J. C. *J. Am. Chem. Soc.* **2009**, *131*, 3878-3880.
38. Carrier, S. M.; Ruggiero, C. E.; Tolman, W. B. *J. Am. Chem. Soc.* **1992**, *114*, 4407-4408.
39. Fujisawa, K.; Tateda, A.; Miyashita, Y.; Okamoto, K.-I.; Paulat, F.; Praneeth, V. K. K.; Merkle, A.; Lehnert, N. *J. Am. Chem. Soc.* **2008**, *130*, 1205-1213.
40. Ruggiero, C. E.; Carrier, S. M.; Antholine, W. E.; Whittake, J. W.; Cramer, C. J.; Tolman, W. B. *J. Am. Chem. Soc.* **1993**, *115*, 11285-11298.